Journal of Tissue Engineering
4: 2041731413492741

DOI: 10.1177/2041731413492741
tej.sagepub.com
SAGE

Cellular distribution and gene expression profile during flexor tendon graft repair: A novel tissue engineering approach*

Subhash C Juneja[1,2]

Abstract

To understand scar and adhesion formation during postsurgical period of intrasynovial tendon graft healing, a murine model of flexor digitorum longus tendon graft repair was developed, by utilizing flexor digitorum longus tendon allograft from donor Rosa26/+ mouse, and the healing process at days 3, 7, 14, 21, 28, and 35 post surgery of host wild-type mouse was followed. Using X-gal staining, β-galactosidase positive cells of allograft origin were detectable in tissue sections of grafted tendon post surgery. Graft healing was assessed for the cellular density, scar and adhesion formation, and their interaction with surrounding tissue. From histological analysis, it was evident that the healing of intrasynovial flexor digitorum longus tendon graft takes place in an interactive environment of donor graft, host tendon, and host surrounding tissue. A total of 32 genes, analyzed by RNA analysis, expressed during healing process. Particularly, *Alk1, Postn, Tnc, Tppp3*, and *Mkx* will be further investigated for therapeutical value in reducing scars and adhesions.

Keywords

Flexor tendon, graft healing, Rosa26/+ mice, scars, adhesion formation

Introduction

Wound healing comprised several phases, which overlap each other (Figure 1). Repair of injuries to flexor tendon is complicated by fibrotic adhesions that compromised postoperative gliding and limit the range of joint flexion.[1] Adhesions are especially exacerbated in injuries involving flexor digitorum profundus and flexor digitorum superficialis tendons in Bunnell's "no man's land" or zone II of the hand.[2] As an alternative to primary repair, which still represents the standard of care for these injuries, surgeons often use a live tendon autograft.[2,3] Unfortunately, the flexor tendon grafting procedures also experience postoperative adhesions that limit joint flexion or cause joint contracture. The biological mechanisms of flexor tendon graft repair and adhesion formation are still poorly understood. Adhesions following live autograft reconstruction are thought to arise through intrinsic or extrinsic fibrosis, among other factors, including gap length, and following postoperative protocols to be considered.[1,4,5] It was hypothesized that the flexor digitorum longus (FDL) tendon graft healing process results from an interactive environment created by the donor FDL tendon allograft, host FDL tendon, and host surrounding tissue. To uncover this, an investigation was made to analyze the interactive cellular and molecular environment. A mouse model was developed in which a 3-mm gap defect was created in FDL tendon of hind limb of a wild-type (WT) mouse, which, in turn, was repaired by replacing with a 3-mm FDL tendon allograft from a Rosa26/+ reporter mouse, and an adequate immobilization to induce robust adhesion formation was also provided. β-galactosidase (β-gal) staining allowed to localize the cells of allograft origin during healing process in an interactive environment of donor allograft, host tendon, and the host surrounding tissue. RNA analysis of interactive environment provided the information of molecular factors that are involved in tendon healing process. This novel murine model will allow us to understand the cellular and molecular mechanisms and will target pharmacological manipulations to devise novel treatments to inhibit

[1]The Center for Musculoskeletal Research, University of Rochester Medical Center, Rochester, NY, USA
[2]Division of Orthopaedic Surgery, Toronto Western Hospital, University Health Network, Toronto, ON, Canada

Corresponding author:
Subhash C Juneja, Division of Orthopaedic Surgery, Toronto Western Hospital, University Health Network, 101 College Street, Max Bell Research Centre, Room #20-1R414, Toronto, ON M5G 1L7, Canada.
Email: Subhash_juneja@urmc.Rochester.edu; sjuneja.phd@gmail.com; sjuneja@uhnresearch.ca

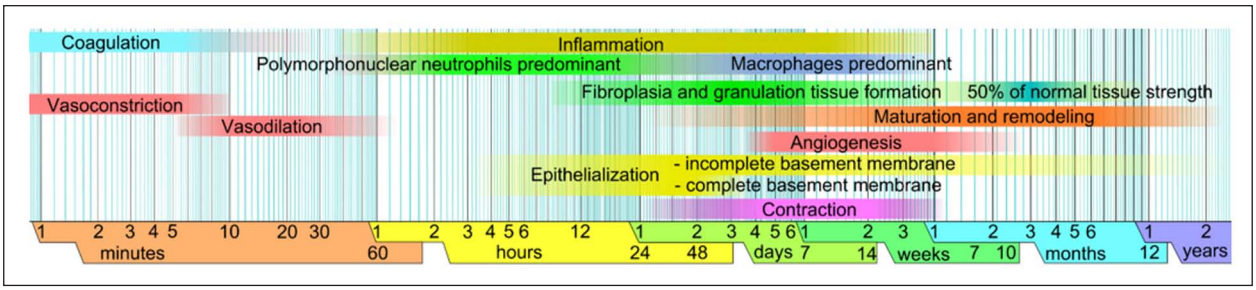

Figure 1. A diagrammatic sketch of wound healing phases.
Source: Graphic created by and courtesy from Mikael Haggstrom, Wikipedia, with permission to use this figure for any purpose.

adhesion and scar formation and will aid to increase mobility of the hand after surgery in human patients.

Materials and methods

Mouse breeding

Transgenic Rosa26/+ ((B6.129S7-*Gt(ROSA)26Sor*/J); stock number: 002192) mice (The Jackson Laboratory, Bar Harbor, ME, USA), which carried retroviral insertion of bacterial *lacZ* (gene for β-gal) at one allele,[6] were used and maintained at B6 (C57BL/6J) background. Het mice served as FDL tendon allograft donor and WT mice served as recipient. Mouse colony was expanded by Het × WT crosses. Genotyping was done by polymerase chain reaction (PCR) using primer sequences (5′ → 3′; oIMR0092: AAT CCA TCT TGT TCA ATG GCC GAT C, oIMR0314: GGC TTA AAG GCT AAC CTG ATG TG, oIMR3449: CCG GAT TGA TGG TAG TGG TC, oIMR8546: GGA GCG GGA GAA ATG GAT ATG). Genotyping protocol was used from mice vendor's website (The Jackson Laboratory). Animal use protocol was approved by the University of Rochester Animal Care Committee. The experiment was divided into two groups: (1) histological studies and (2) messenger RNA (mRNA) expression.

Surgical procedures

At each time-point, three surgeries were performed for histological analysis and six surgeries were performed for RNA expression analysis on 3-month-old mice. Mice were anesthetized using intraperitoneal (ip) injection of ketamine (60 mg/kg of body weight) and xylazine (4 mg/kg of body weight). Surgeries were performed at 4.9× magnification eye loupes (Surgical Acuity, Middleton, Wisconsin, USA) and using microsurgical background material (Accurate Surgical and Scientific Instruments Corporation, Westbury, NY, USA). Briefly, a longitudinal plantar incision was created on the hind foot of a WT mouse. A 3-mm defect was created in FDL tendon of WT mouse and filled by suturing a 3-mm FDL tendon allograft from Rosa 26/+ mouse using a 9-0 ETHILON™ suture (monofilament nylon, tapercut V100-3; Ethicon, Inc, Somerville, New Jersey, USA) and utilizing a modified Kessler technique (Figure 2(a) to (b)). The tendon was then transected at the proximal musculotendinous junction to temporarily immobilize the flexion mechanism to protect against disruption of the tendon graft early during the repair period and to eliminate early tendon gliding to induce adhesion formation. The skin was closed using 5-0 ETHILON nylon suture (668G, Ethicon). Mice were sacrificed at different time-points between days 3 and 35 post surgery for histological studies and for RNA expression studies. The overall plan of the study is shown in Figure 2(c). The unoperated FDL tendon tissue was recovered from WT mice without grafting and repair for histological comparison.

Histological studies

Mice were sacrificed using CO_2 anesthesia followed by decapitation and tissues were recovered. Tendon tissue was dissected along with surrounding tissue with a scalpel. The tissue was fixed in 3 mL of freshly diluted cold 4% paraformaldehyde (PFA) (methanol-free formaldehyde, EM Sciences) for 1 h, washed with cold phosphate buffered saline (PBS) three times for 10 min each, transferred to cold 15% sucrose solution (in PBS) with gentle rocking for 3 h, and finally transferred to 30% sucrose and kept overnight in a cold room at 5° with gentle rocking. The tissue was rinsed thrice, 5 min each in optimal cutting temperature (OCT) compound/freezing medium (Tissue-Tek®), and placed in a Cryomold® (Tissue-Tek) filled with OCT. Semi-thin sections of 7 µm thickness were cut using a Cryostat (Thermo, Hanover Park, Illinois, USA) and Accu-Edge® blades (Sakura, Torrance, California, USA).

X-gal staining

Frozen sections were stained for β-gal using X-gal as a substrate (Invitrogen, Carlsbad, California, United States). Briefly, frozen slides were warmed to 4°C, fixed in cold freshly diluted (in PBS) 0.2% glutaraldehyde (EM Sciences) for 10 min, and washed once in PBS, once in wash solution (PBS containing 2-mM $MgCl_2$ and 0.02% NP-40), and once in staining solution (wash solution containing 5-mM $K_4Fe(CN)_6$ and 5-mM $K_3Fe(CN)_6$) for 5 min each. Finally, slides were placed in a

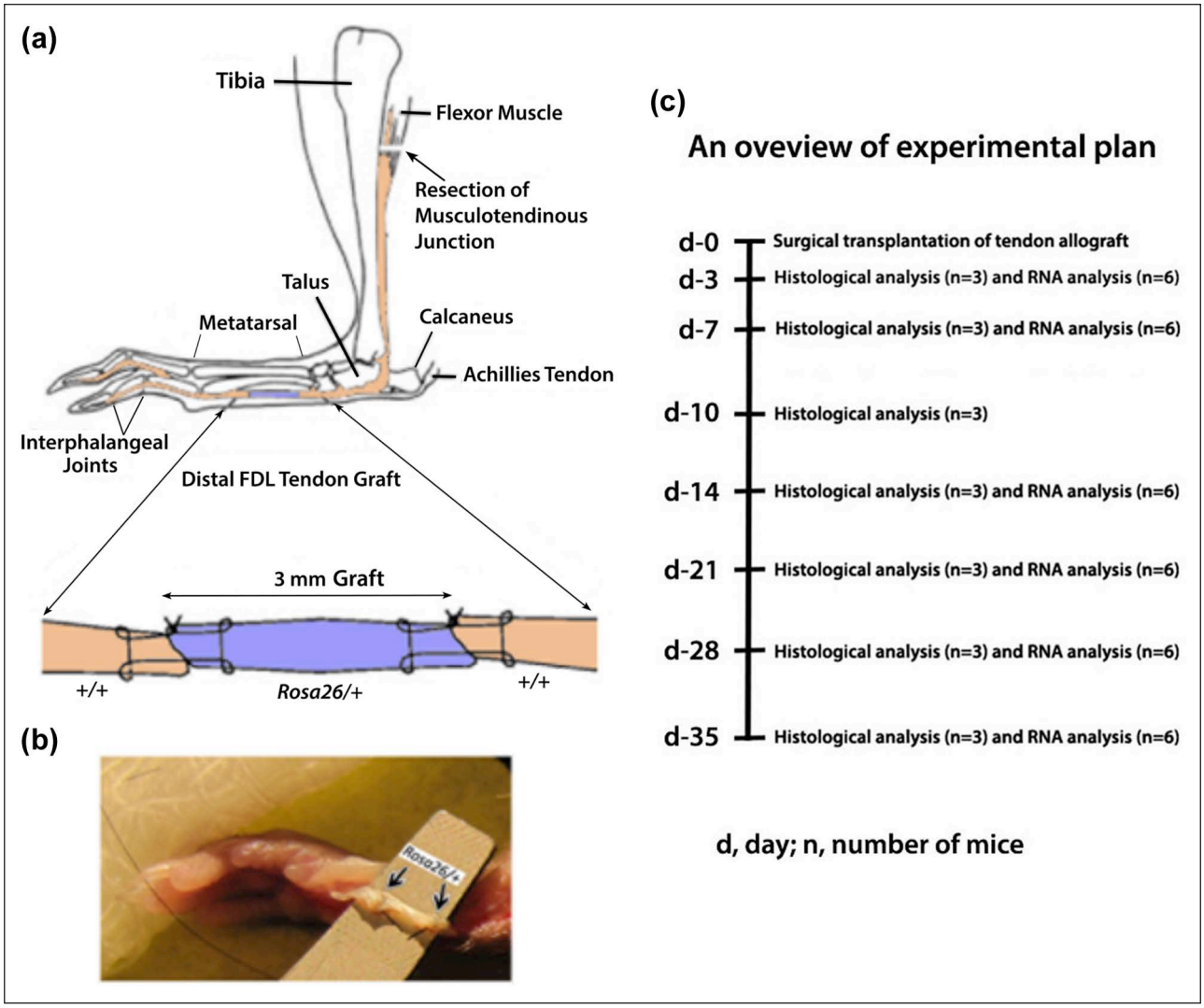

Figure 2. (a) (Top) (reproduced with permission from John Wiley and Sons,[7] modified): a schematic illustration of the live allograft reconstruction of murine distal FDL tendon. A 3-mm gap defect in distal FDL tendon in the hind foot of wild-type mouse was created and replaced surgically by a 3-mm FDL tendon allograft from Rosa26/+ mouse using 9-0 ETHILON™ suture with modified Kessler technique. The tendon is transected at the proximal musculotendinous junction (arrow) to temporarily immobilize the flexion mechanism to protect against the disruption of the tendon graft and to stimulate adhesions. (b) (Bottom): a 3-mm gap in the hind foot of wild-type mouse replaced surgically by a 3-mm live allograft (between arrows) from Rosa26/+ mouse. (c) An overview of experimental plan is shown.
FDL: flexor digitorum longus.

Coplin jar containing "working solution" of X-gal (5-bromo-4-chloro-3-indolyl-β-D-galactopyranoside) substrate at 1 mg/mL of staining solution. The slides were placed at 35°C for 8 h for color development. The slides were rinsed twice in PBS for 15 s each time, given pinkish/red background by placing the slides in "nuclear fast red solution" (EM sciences) for 10 min, rinsed in PBS, and then dehydrated by passing twice through increasing concentration of ethanol solutions (70%, 95%, 100%) for 5 min each time. The sections were cleared by passing through xylene (Fisher Scientific, Canada) twice, for 5 min each time, mounted permanently with a Cytoseal 60 (Thermo), a mounting medium, and photographed under light microscope (Zeiss, Oberkochen, Germany). Photographs of representative histological sections are shown in the results (Figure 3).

Hematoxylin and eosin staining

Frozen sections of FDL tendon from unoperated mice were stained with hematoxylin and eosin (H&E) only. Briefly, frozen slides were warmed to 4°C, fixed in cold freshly diluted (in PBS) 0.2% glutaraldehyde (EM Sciences) for 10 min, and washed once in PBS and then once with distilled water. The sections were treated with a series of solutions—hematoxylin (for 4 min, for nuclei

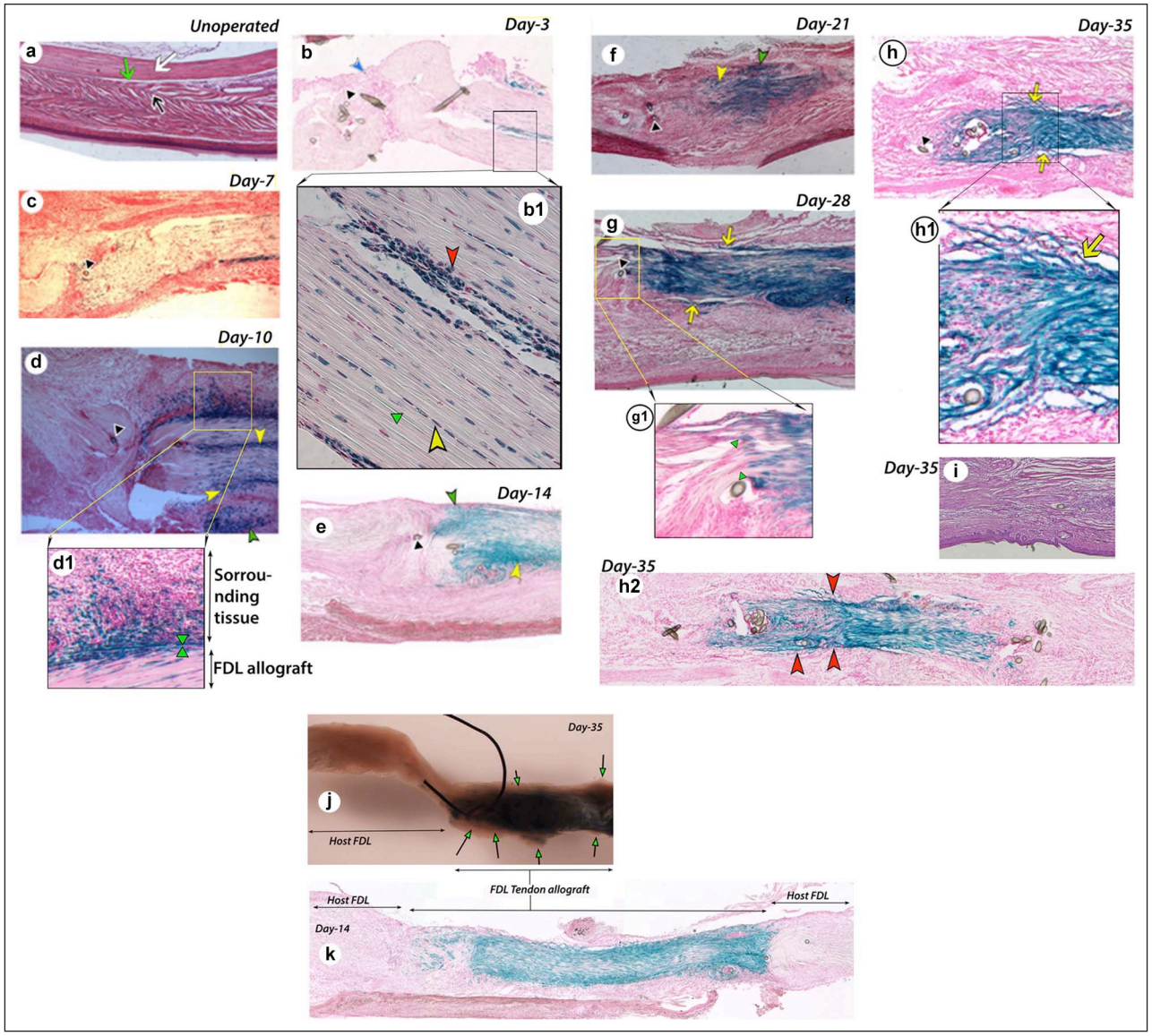

Figure 3. (a) Histology of FDL tendon. Hematoxylin and eosin–stained section of an unoperated FDL tendon shows intact FDL tendon (white arrow), surrounding tissue (black arrow), and gliding space (green arrow). X-gal-stained and nuclear fast red-stained frozen sections of FDL tendon graft tissue with surrounding tissue at different days post surgery: (b) day 3, (c) day 7, (d) day 10, (e) day 14, (f) day 21, (g) day 28, (h) day 35, and (h2) day 35, full length tendon graft at a different plane than (h). (i) Hematoxylin and eosin–stained section of day 35 tendon graft. (j) Whole mount of tendon graft pulled out forcibly from its surrounding tissues. (k) Full-length day 14 tendon graft. Higher magnification images of (b1) day 3, (d1) day 10, (g1) day 28, and (h1) day 35.
FDL: flexor digitorum longus.
(b) Inflammatory cell mass, blue arrowhead; (d–f) scar tissue, yellow arrowhead; (d–f) invasion of cells of allograft origin into surrounding sheath and tissue, green arrowhead; (g, h) adhesions, yellow arrow; (b–h) suture remnants, black arrowhead; (b1) red arrowhead shows more cells at the periphery and also more cells round in shape, yellow arrowhead shows elongated tenocyte cells well aligned within collagen fibers, and green arrowhead indicates aligned collagen fibers; (d1) green arrowheads mark the approximate demarcation of grafted donor tendon and host surrounding tissue; of the note, blue color cells from donor tendon graft have migrated well deep in the host surrounding tissue; (g1) green arrowheads show the demarcation where host and donor collagen fibers align and allow healing of tendon graft per say; (h1) yellow arrow indicates adhesion between donor tendon allograft and the host surrounding tissue at day 35; (h2) red arrowheads indicate relatively more adhesions, adhesions are more in (h2) than (h) in a section at different plane at day 35; (j) arrows with green head show the adhesions and some tissues (nonblue) at the periphery pulled from the host surrounding tissues at day 35; (k) host FDL shows no staining, whereas FDL tendon allograft shows the blue staining, indicating that host FDL can serve as a good negative control and there is no nonspecific blue staining in that area.

staining; Sigma-Aldrich, St. Louis, Missouri, USA, product no. H3136), rinsed gently in running tap water, dipped in 0.3% acid alcohol for 1 min, dipped twice in tap water briefly, stained with eosin for 2 min, and again dipped in tap water briefly. The slides were dehydrated and mounted permanently as described earlier.

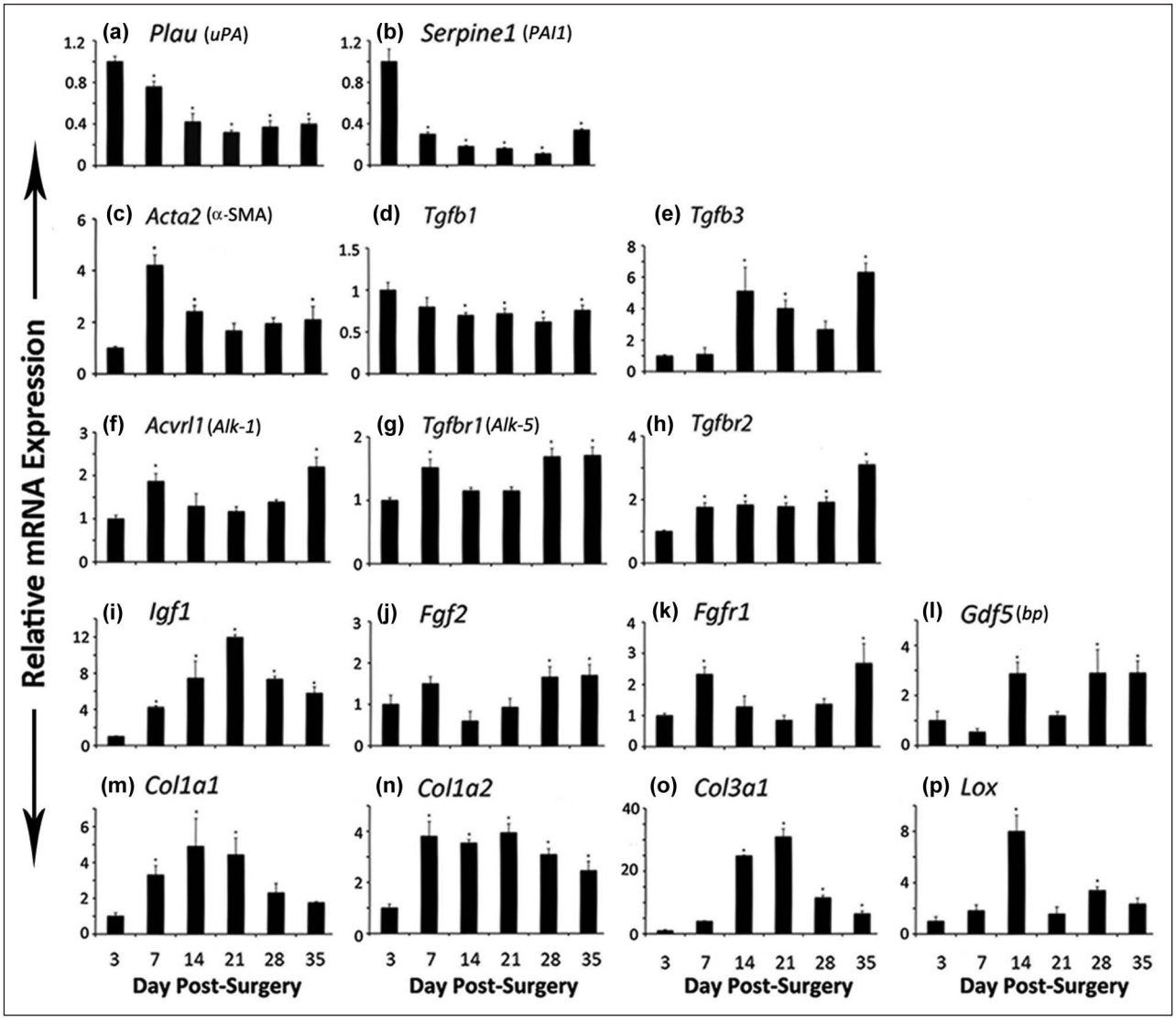

Figure 4. mRNA expression of (a) *Plau* or *uPA*, (b) *Serpine1 or PAI1*, (c) *Acta2 or α-SMA*, (d) *Tgfb1*, (e) *Tgfb3*, (f) *Acvrl1 or Alk-1*, (g) *Tgfbr1 or Alk-5*, (h) *Tgfbr2*, (i) *Igf1*, (j) *Fgf2*, (k) *Fgfr1*, (l) *Gdf5 or bp*, (m) *Col1a1*, (n) *Col1a2*, (o) *Col3a1*, and (p) *Lox* genes at different days of FDL tendon graft healing at days 3, 7, 14, 21, 28, and 35.
FDL: flexor digitorum longus; SD: standard deviation; RT-PCR: reverse transcription polymerase chain reaction; *α-SMA*: alpha-smooth muscle actin. Total RNA was extracted from tendon and surrounding tissue from six mice and processed for real-time RT-PCR. Gene expression was standardized with the internal *β-actin* control and then normalized by the level of expression at day 3 post surgery. Data are presented as the mean fold induction (over day 3 surgery) and ±SD; *$p < 0.05$ or less considered significantly different from day 3.

RNA extraction and real-time reverse transcription polymerase chain reaction

For total RNA isolation, the tissue consisted of 1.5 mm of sutured weave of tendon-allograft junctions on each side. The tissue included FDL tendon along with its surrounding tissue. Samples at each time-point from six animals were pooled in a sterile tube containing 20 mL of RNAlater® solution (Invitrogen) at room temperature. The tissue pieces were transferred to TRIzol® reagent (Invitrogen) and homogenized using a hand-driven glass homogenizer, and total RNA was isolated using manufacturer's protocol. Complementary DNA (cDNA) was prepared from 1 μg total RNA in a 20 μL of reaction mixture in 0.2-mL tubes (Bio-Rad) using MMLV Reverse Transcriptase system (Invitrogen) and following the manufacturer's protocol. A fixed volume of 0.5 μL of cDNA was used for real-time reverse transcription polymerase chain reaction (RT-PCR) using SYBR Green (Applied Biosystems, Foster City, California, USA) and specific primers for mouse genes (Supplementary Table S1). mRNA expression of several genes at different time-points was assessed (Figures 4 and 5). The amplification was monitored real time using the 96-well iCycler iQ™ Real-Time PCR Detection System (Bio-Rad, Hercules, California, USA). The threshold cycle (C_t) values were related to a standard curve made with the

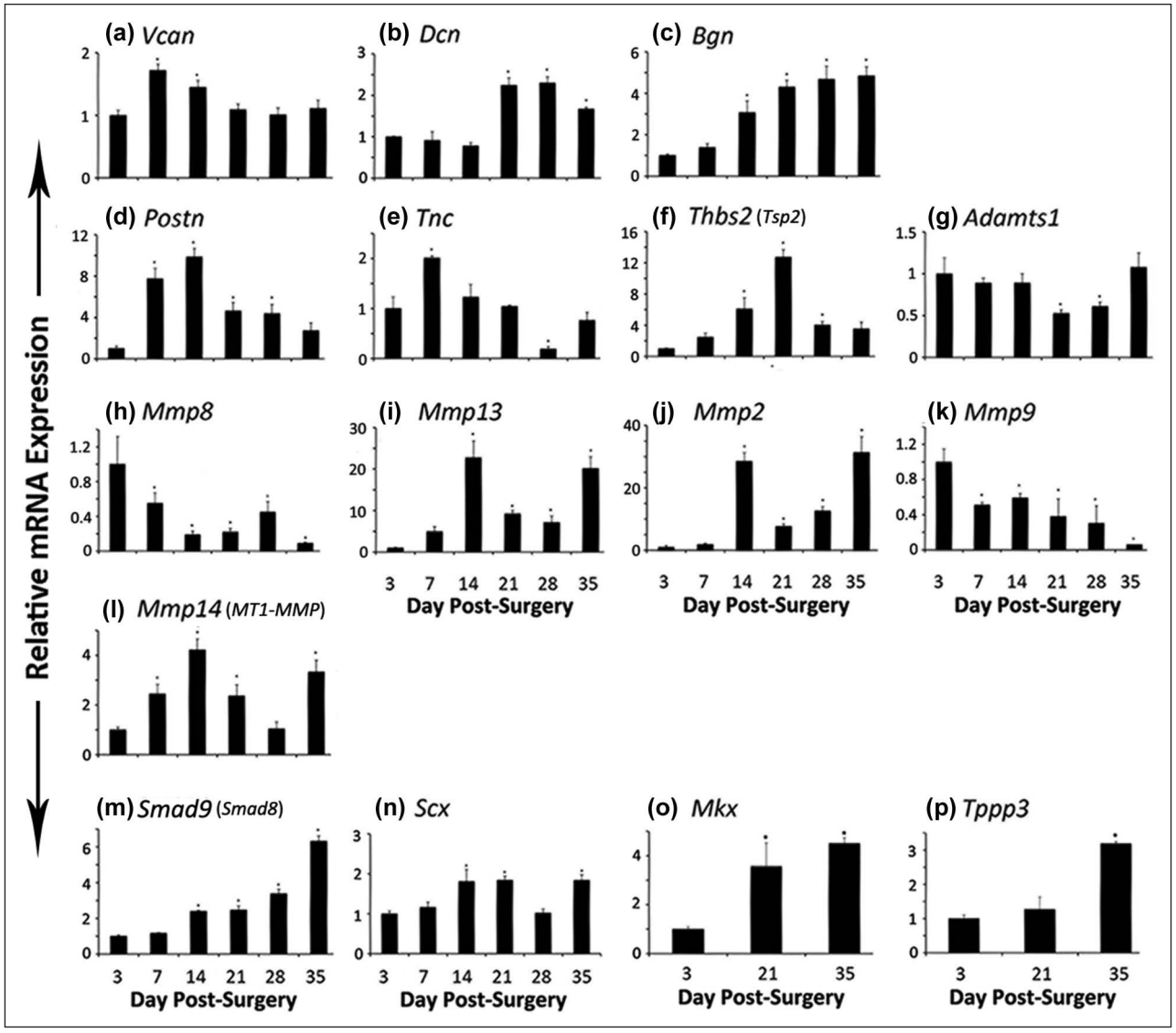

Figure 5. mRNA expression of (a) *Vcan*, (b) *Dcn*, (c) *Bgn*, (d) *Postn*, (e) *Tnc*, (f) *Thbs2 or Tsp2*, (g) *Adamts1*, (h) *Mmp8*, (i) *Mmp13*, (j) *Mmp2*, (k) *Mmp9*, (l) *Mmp14 or MT1-MMP*, (m) *Smad9* or *Smad8*, and (n) *Scx* genes at different days of FDL tendon graft healing at days 3, 7, 14, 21, 28, and 35. mRNA expression of (o) *Mkx* and (p) *Tppp3* was also assessed at days 3, 21, and 35.
FDL: flexor digitorum longus.
Total RNA was extracted from tendon and surrounding tissue from six mice and processed for real-time RT-PCR. Gene expression was standardized with the internal β-*actin* control and then normalized by the level of expression at day 3 post surgery. Data are presented as the mean fold induction (over day 3 surgery) and ±SD; *p < 0.05 or less considered significantly different from day 3.

cloned PCR products, and specificity was confirmed by melting curve analysis after amplification. The general range of C_t values was 15–30. Beta-actin gene *Actb* was chosen as an internal control expressed. Data at different time-points, in quadruplicates, are presented as the mean fold induction over day 3 post surgery; ± standard deviation (SD); p value less than 0.05 differing from day 3 counterpart, was considered as significantly different. Experiment was repeated three times to observe the consistency of RNA data. Data were analyzed using one-way analysis of variance (ANOVA) followed by Tukey's all-pair comparisons at $\alpha = 0.05$. A computer software KaleidaGraph was used to analyze the data and MS office Excel was used to draw graphs.

A cohort of genes was considered for the analysis in this study assuming that these will play a role in tendon graft healing. That included the following: fibrinolysis (*Plau or uPA, Serpine1 or PAI-1*), inflammation (*Tgfb, Mmp8*), provisional extracellular matrix (ECM) proteoglycan (*Vcan*), wound contraction (*Acta2*), regulation of deposition of ECM and fibrosis (*Tgfb1, Tgfb3*, and receptors *Acvrl1* or *Alk-1, Tgfbr1* or *Alk-5*, and *Tgfbr2*), tendon tensile strength ECM (*Col1a1, Co11a2, Col3a1*), tendon healing and regeneration (*Igf1*), tendon fibroblast growth (*Fgf2* or *bFgf* and

receptor *Fgfr1*), neotendon formation (*Smad8* or *Smad9*), neotendon formation and tendon healing (*Gdf5*), tenocyte differentiation and markers (*Scx* and *Mkx*), collagen fibrillogenesis (*Dcn and Bgn*) and cross-linking (*Lox*), regulation under constant mechanical stress (*Postn*), regulation of tensile strength (*Tnc*), remodeling (*Mmp2, Mmp9, Mmp14* and *Adamts1*), tendon peripheral protein (*Tppp3*), and vasculogenesis (*Thbs2* or *Tsp2*).

Results

Histological assessment of FDL tendon graft

Figure 3(a) shows H&E staining of FDL tendon sections from an unoperated mouse, which represents intact FDL tendon with parallel collagen fibrils and the surrounding tissue with a narrow space between them for gliding. Figure 3(b) to (h) shows X-gal-stained sections from grafted FDL tendon at different time-points post surgery (days 3, 7, 10, 14, 21, 28, and 35). The β-gal positive cells of allograft origin are present at all the time-points post surgery (Figure 3(b) to (h)). The density of β-gal positive cells in the grafted tendon is lower at days 3 and 7 (Figure 3(b) and (c)) as compared to other days (day 10 through day 35, Figure 3(d) to (h)). The density increased intensely at day 10 (Figure 3(d)). The β-gal positive cells are present in scars (Figure 3(d) to (f)) and in adhesions (Figure 3(g) and (h)) and show invasion into its surrounding tissue (Figure 3(d) to (f)). Figure 3(j) shows the whole mount of grafted tendon forcibly separated from surrounding tissues, which indicates a number of adhesion areas in the healing grafted tendon. Figure 3(k) clearly shows that host tendon was not stained positive for β-gal staining, whereas donor allograft tissue was stained with blue staining. Figure 3(i), which presents a section stained with H&E alone, does not provide better view of healing tendon graft than β-gal-stained tissue.

At higher magnification, day 3 healing graft shows that tendon cells at the periphery become more round and probably participate in cell division (Figure 3(b1)). Tendon tissue at day 10 reveals how interactive environment is created by the healing tissues. Tendon graft β-gal positive cells show invasion in the surrounding tissues of tendon (Figure 3(d1)). Interestingly, day 28 tendon shows the boundary between the grafted tendon and host tendon tissues and the continuity of collagen fibers (Figure 3(g1)). Adhesions are visible between host surrounding tissue and donor tendon allograft (Figure 3(h1)). Tissue section at different planes differs in the extent of adhesion area. Figure 3(h2) presents another plane than that of Figure 3(h) and shows that this plane has more adhesions than Figure 3(h).

Fibrinolysis regulation

Expression of *Plau* (plasminogen activator, urokinase)/*uPA* (urokinase-type plasminogen activator) and *Serpine1* ((serine (or cysteine) peptidase inhibitor, clade E, member 1))/PAI1 (plasminogen activator inhibitor 1) mRNA was highest at day 3 post surgery, which gradually decreased by day 35 and was significantly lower at each time-point as compared to day 3 (Figure 4(a) and (b)).

Wound contraction

Expression of *Acta2* (actin, alpha 2, smooth muscle, aorta)/*α*-smooth muscle actin (α-SMA) mRNA remained elevated on all the time-points as compared to day 3, showing significantly higher levels at days 7, 14, and 35, the day 7 with the highest peak level (Figure 4(c)).

Transforming growth factor βs and receptors

Expression of *Tgfb1* (transforming growth factor (TGF), beta 1) mRNA showed highest level at day 3 (Figure 4(d)). The levels decreased steadily and were significantly lower at days 14, 21, 28, and 35, whereas *Tgfb3* (TGF, beta 3) mRNA expression showed a reverse and an increasing trend in its expression, the levels being significantly higher at days 14, 21, and 35 and nonsignificantly higher at day 28 (Figure 4(e)). Expression of *Acvrl1* (activin A receptor, type II-like 1)/*Alk-1* mRNA increased significantly at days 7 and 35 and remained nonsignificantly higher at all the other time-points as compared to day 3 (Figure 4(f)), whereas *Tgfbr1* (TGF, beta receptor I)/*Alk-5* expression showed a significant increase at days 7, 28, and 35 (Figure 4(g)). Expression of *Tgfbr2* (TGF, beta receptor II) was significantly higher at all the time-points as compared to day 3 (Figure 4(h)).

Growth factors

Gene expression of *Igf1* (insulin-like growth factor 1) mRNA upregulated significantly at all the time-points with peak level at day 21 as compared to day 3 post surgery (Figure 4(i)). There was a nonsignificant increase in *Fgf2* (fibroblast growth factor 2)/*bFGF* (basic FGF) mRNA expression at day 7 and significant increase at days 28 and 35 (Figure 4(j)), whereas *Fgfr1* (fibroblast growth factor receptor 1) mRNA expression was significantly higher at days 7 and 35 (Figure 4(k)). Gene expression of growth differentiation factor 5 (*Gdf5*)/brachypodism (*bp*) mRNA was significantly higher at days 14, 28, and 35 (Figure 4(l)).

Collagens and lysyl oxidase

Gene expressions of *Col1a1* (collagen, type I, alpha 1), *Col1a2* (collagen, type I, alpha 2), and *Col3a1* (collagen, type III, alpha1) mRNA show an increase during healing period (Figure 4(m) to (o)): *Col1a1* expression increased significantly at days 7, 14, and 21 and remained nonsignificantly higher at days 28 and 35 (Figure 4(m)), whereas *Col1a2* expression was significantly higher at

all the time-points as compared to day 3 expression (Figure 4(n)). Expression of *Col3a1* mRNA followed a sharp increase and then a sharp decrease pattern (Figure 4(o)). Lysyl oxidase (*Lox*) expression showed a sharp increase at day 14 and second smaller peak at day 28 (Figure 4(p)).

Proteoglycans

Expression of *Vcan* (versican) mRNA was significantly higher at days 7 and 14 and then declined, whereas *Dcn* (decorin) mRNA expression was significantly higher at days 21, 28, and 35 (Figure 5(a) and (b)). They appear to show a complementary role during healing period. Biglycan (*Bgn*) showed significantly higher expression at days 14, 21, 28, and 35 (Figure 5(c)). Periostin (*Postn*) expression was significantly higher at day 7 and remained significantly higher until day 28 (Figure 5(d)), and tenascin C (*Tnc*) showed significantly higher peak level at day 7 (Figure 5(e)).

Glycoprotein

Thrombospondin 2 (*Thbs*2)/*Tsp2* expression remained higher at all the time-points with significantly increased level only at days 14, 21, and 28 (Figure 5(f)).

Matrix remodeling enzymes

The expression of *Adamts1* (a disintegrin-like and metallopeptidase (reprolysin type) with thrombospondin type 1 motif, 1) mRNA showed a reverse trend than that of *Thbs2*, being significantly lower at days 21 and 28 (Figure 5(g)). Matrix metallopeptidase 8 (*Mmp8*)/collagenase-2 mRNA expression was maximum at day 3 and then decreased significantly at all the other time-points (Figure 5(h)). Matrix metallopeptidase 13 (*Mmp13*)/collagenase-3 expression shows two major significantly higher peaks at days 14 and 35 as well as two minor but significantly higher peaks at days 21 and 28 (Figure 5(i)). Matrix metallopeptidase 2 (*Mmp2*/gelatinase A) mRNA expression showed significantly higher level with larger peaks at days 14 and 35 and smaller peaks at days 21 and 28 (Figure 5(j)), whereas *Mmp9* (matrix metallopeptidase 9/gelatinase B) mRNA expression level was highest at day 3 and then decreased at all the time-points significantly (Figure 5(k)). Matrix metallopeptidase 14 (membrane-inserted)/*Mmp14*/MT1-MMP expression was significantly higher at days 7, 14, 21, and 35 as compared to day 3 expression (Figure 5(l)).

Developmental/progenitor/differentiation factors

The expression of mothers against decapentaplegic homolog 9 (*Smad9*, MAD homolog 9 (Drosophila) or its synonym, *Smad8*) mRNA expression increased significantly at day 14 onwards at each time-point as compared to day 3 expression (Figure 5(m)). Scleraxis (*Scx*) expression was significantly higher at days 14, 21, and 35 (Figure 5(n)). Mohawk homeobox (*Mkx*) gene expression, studied at three time-points, was significantly higher at days 21 and 35 as compared to day 3 expression (Figure 5(o)).

Cell matrix protein

Tubulin polymerization-promoting protein 3 (*Tppp3*) mRNA expression, studied at three time-points, was significantly higher at day 35 and nonsignificant at day 21 as compared to day 3 post surgery (Figure 5(p)).

Discussion

Histological assessment of FDL tendon graft

To understand scar and adhesion formation during postsurgical period of intrasynovial tendon, a murine model of FDL tendon graft repair was developed, by implanting the FDL tendon allograft from Rosa26/+ mouse into WT mouse, and the healing process from day 3 through day 35 at different time-points post surgery was followed. Using X-gal staining, β-gal positive cells of allograft origin were detectable in frozen sections of grafted tendon, recovered at different time-points post surgery. β-gal positive cells were at low cell density in grafted allograft during early phase of healing, indicating apoptotic events at days 3 and 7 (Figure 3(b) and (c)), though cells proliferated rapidly by day 10 (Figure 3(d)) onward. Apoptosis in the healing tendons peaks at day 3, followed about 10 days later by the peak proliferation period.[8] It is also obvious that the cells from grafted tendon invaded deep into the surrounding tissue at days 10, 14, and 21 as shown by β-gal positive cells (Figure 3(d) to (f)), indicating that the healing process occurred in the presence of factors that are contributed by tendon and surrounding tissue, that is, in an interactive environment. The cell biology of flexor tendon healing follows the classic wound healing response of inflammation, proliferation, synthesis, and apoptosis, but the greater activity occurs in the surrounding tissue.[9] Based on histological observations, gene expression was analyzed from the tissues collected from grafted FDL tendon along with its surrounding tissue. Hence, the current investigation presents gene expression data based on the interactive environment. It is shown that the tendon cells invade much deeper into the surrounding tissue than previously believed, and hence, the role of surrounding tissue cannot be ignored during healing process. Additionally, the current mouse model will provide simple histological assessment of scars (Figure 3(d) to (f)) and adhesions (Figure 3(g) and (h)) in an experimental setting. As shown by β-gal staining of whole mount of isolated tendon graft and histological section (Figure 3(j) and (k)), donor tendon

allograft has well maintained its cellular density as indicated by the blue coloration. The study indicates that healing occurred by cellular contribution from both host and donor tendon. In contrast, in rat Achilles tendon-bone insertion graft healing study, using LacZ donor tendon or LacZ host bone, the authors showed that the healing of insertion was due to host cells rather than donor tendon cells.[10] The reason could be that in Kobayashi et al.'s[10] experiment, the study is based on tendon-bone insertion healing. These two systems should be considered completely different. There is possibility that tendon cells need to change to next differentiated stage to cross talk with cells at the insertion site in Kobayashi's study. And only cells from host may provide that. Or there could be more inflammation at tendon-bone insertion during healing and cells from tendon might have undergone apoptosis due to heavy inflammation.[10] Other but yet unknown reasons for the difference between this study and the Kobayashi's study cannot be ruled out.[10]

Gene expression in grafted FDL tendon

Urokinase-type plasminogen activator (*Plau* or *uPA*) plays a vital role in the early phases of wound healing by aiding fibrin dissolution, promoting the migration, proliferation, and adhesion of various cells to the wound bed.[11] In wounded gingival granulation tissue, Tgfβ1 caused an enhanced expression of uPA in cells expressing α-SMA indicating its role during wounds.[12] Expression of *uPA* mRNAs was maximal at days 4 and 7 following Achilles tendon injury.[13] In this study, *Plau* mRNA expression was highest at day 3 (Figure 4(a)), indicating its role in early phase of healing, in which uPA activates the conversion of plasminogen to plasmin, which in turn degrades unwanted fibrin deposited in blood clot and other remodeling functions (i.e. activation of MMPs). The study indicates that uPA plays a role in FDL tendon graft healing process.

Plasminogen activator inhibitor 1 (SERPINE1/PAI-1), a single-chain glycoprotein, which is present in plasma as well as synthesized by many tissues, inhibits uPA and tPA (tissue plasminogen activator) and is therefore a regulator of plasminogen activation and plays primary role in fibrinolysis and also involved in the regulation of cell adhesion, cell migration, and invasion.[11] Skin wound healing is accelerated in PAI-1-deficient mice.[14] Highest level of *Serpine1* mRNA expression at day 3 indicates its role during inflammation (Figure 4(b)).

Alpha-actin-2 (*Acta2* (*α-SMA*) (actin isoform, α-SMA)), though mainly expressed in muscle tissues, has been identified in fibroblastic cells of normal tendons, ligaments, and myofibroblasts.[15] Alpha-actin-2-expressing cells (myofibroblasts), in injured rabbit ligament (day 3 to 12 weeks post injury), were identified at day 3 in medial collateral ligament, and their density increased steadily to day 21.[16] In FDL tendon graft healing, *Acta2* mRNA expression remained higher on all the days as compared to day 3 post surgery indicating its role in all the postinflammatory events (Figure 4(c)). The highest level at day 7 indicates its major role in contraction events of healing aiding closing of the wound (Figure 4(c)). In the sheep's anterior cruciate ligament with Achilles tendon graft, the midsubstance tissue samples stained for α-SMA indicate the presence of myofibroblasts at 6 weeks post surgery within the newly formed fiber bundles.[15]

TGFβ1 and TGFβ3 (encoded by genes *Tgfb1* and *Tgfb3*, respectively) play a central role in regulating wound repair, by acting as a molecular switch, turning on or off the deposition and accumulation of ECM in the wound area. This enhanced accumulation of ECM is the result of TGFβ's ability to regulate synthesis of ECM, proteases, protease inhibitors, and integrins resulting in increased adhesion to ECM. While these events are beneficial in terms of wound repair, the TGFβ-induced ECM deposition, if not switched off, can lead to the negative side of healing process, that is, scarring and fibrosis.[17] In the current murine FDL tendon graft healing study, *Tgfb1* mRNA expression showed highest level during inflammatory phase and the level steadily declines by day 35 (Figure 4(d)), whereas *Tgfb3* showed a reverse and an increasing trend in its expression over healing period, the strong induction particularly at later stages of healing process (Figure 4(e)). Skin wound repair shows that *Tgfb1* mRNA expression decreased from day 3 until day 13 but *Tgfb3* expression increased from day 3 until day 13 in a 13-day study.[18] TGFβ3 has been shown to reduce connective tissue deposition and subsequent scarring during wound healing in normal rats.[19]

Through the receptors (*Acvrl1* (*Alk-1*), *Tgfbr1* (*Alk-5*), and *Tgfbr2*), TGFβs signal by the ligand (TGFβ1, β2, or β3) binding to its constitutively active TGFβ receptor, type II or TGFR-2 (encoded by *Tgfbr2*), which phosphorylates the TGFβ receptor, type I. Out of a number of TGFβ receptors, type I, the two (ALK-5, encoded by *Tgfbr1* or *Alk-5*, and ALK-1 encoded by *Acvrl1* or *Alk-1*) of them are known to be involved in TGFβ1 signaling.[20] Expression of *Tgfbr2* mRNA remained consistently higher on all the days, whereas *Acvrl1* (*Alk-1*) showed increased expression at days 7 and 35 and *Tgfbr1* (*Alk-5*) showed increased expression at days 7, 28, and 35 (Figure 4(f) to (h)). It is evident that the expression profile of *Alk-1* and *Alk-5* appears similar but their signaling routes (via Smad1/5 or Smad2/3) and target cells (endothelial cells (ECs) or fibroblasts) are different. In fibroblasts, TGFβ signals mainly through ALK-5/Smad-2/3 pathway.[19] Signaling of TGFβ through ALK-5 leads to inhibition of EC proliferation and migration, whereas signaling of TGFβ through ALK-1 induces EC proliferation and migration.[21] Mutations in ALK-1 are linked to hereditary hemorrhagic telangiectasia 2 in human.[22] In the skin wound healing study, in *Alk-1-LacZ* mouse, β-gal expression was found in newly formed blood vessels at days 3 to 8 in a 10-day study, indicating its role during

angiogenesis.[23] It appears that higher levels of mRNA expression of *Acvrl1* (which encodes ALK-1) are responsible for angiogenesis and higher levels of *Tgfbr1* (which encodes ALK-5) are responsible for granular tissue formation, ECM production, maturation, and remodeling during FDL tendon graft healing studies. In rabbit flexor tendon injury, using immunohistochemistry, both the TGF-β receptor types I and II showed highest expression in epitenon and the tendon sheath.[24]

Insulin-like growth factor (IGF-I) has been shown to play a role in wound healing and regeneration. Expression levels of *Igf1* mRNA and protein increased in healing rabbit medial collateral ligament[25] and in canine flexor tendon after laceration.[26] Upregulated *Igf1* mRNA expression, during day 7 through day 35 (Figure 4(i)), indicates that it may play a role in angiogenesis and growth of cells of FDL tendon graft healing. During healing of deep flexor tendon repair in rabbit, *Igf1* mRNA expression was higher in tendon and sheath on all the time-points (days 6 to 42) as compared to day 3.[27]

Fibroblast growth factor 2 (FGF2 or basic FGF) is one of the paracrine FGF1/2/5 subfamilies.[28] The importance of these factors in wound healing was revealed, in part, by the finding that knocking out of *Fgf2* delays reepithelialization in skin wounds.[29] One molecule of FGF2 binds to two molecules of FGF receptor-1 (FGFR1) in the presence of heparan sulfate, and the signaling leads to fibroblast growth.[28] Controlled release of bFGF and platelet-derived growth factor (PDGF)-BB has been shown to be beneficial to tendon repair.[30] Gene transfer in healing flexor tendon through "adeno-associated virus2-bFGF" transduction, an increase in tensile strength was observed.[31] This study showed that *Fgf2* mRNA expression was initially increased at day 7 during granular tissue formation and then mainly at days 28 and 35, indicating its role on cell growth on those days (Figure 4(j)). Interestingly, but not surprisingly, *Fgfr1* mRNA expression profile was more or less similar to *Fgf2* mRNA expression (Figure 4(j) and (k)). This study clearly indicates that FGF2/FGFR1 signaling is required in FDL tendon graft healing.

Growth/differentiation factor 5 (GDF-5 or brachypodism (bp)) belongs to bone morphogenetic proteins (BMPs) family, which is composed of multifunctional growth factors that belong to TGFβ superfamily.[32] GDF-5 implanted ectopically resulted in the formation of neotendon and ligament.[33] It has been shown to play multiple roles in tendon biology and wound healing studies.[34] Application of GDF-5 in two doses enhanced mechanical strength in transected healing Achilles tendon in rat.[35] Tendon healing is delayed in brachypodism mouse ($Gdf5^{bp\text{-}J/bp\text{-}J}$) lacking GDF-5 due to mutation in the gene.[36] This study showed a significant increase in *Gdf5* mRNA expression indicating that GDF-5 plays a role in FDL tendon graft healing (Figure 4(l)).

Collagens contribute tensile strength to tendon and other tissues. Collagen, type I or $[\alpha1(I)]_2\alpha2(I)$ and type III or $[\alpha1(III)]_3$, plays an important role in tendon healing process. During wound healing, one of the fibroblasts' dominant role is the production of collagen. Higher gene expression of all the collagen genes (*Col1a1, Col1a2*, and *Col3a1*; Figure 4(m) to (o)) indicates their role during maturation and remodeling phase of FDL tendon graft healing. In a rat flexor tendon healing study, COL I mRNA expression increased from days 3 to 28 with a peak at day 28, whereas COL III expression increased from day 3 to the peak value at day 14 and then sharply decrease.[37] Healing tendon lesions from horses euthanized 1, 2, 4, 8, or 24 weeks following injury, gene expression using Northern blot, collagen types I and III increased by week-1 following injury and remained elevated throughout the course of the study, though COL I dominated through the period.[38]

Lysyl oxidase (LOX) initiates the cross-linking of lysine-derived aldehyde and plays a role in maturation of collagen. In the current FDL tendon graft healing study, *Lox* mRNA expression showed 8-fold increase at day 14 and 3.5-fold increase at day 28 (Figure 4(p)). The peak *Lox* level at day 14 corresponds to the higher level of mRNA expression of collagen genes (*Col1a1, Col1a2*, and *Col3a1*) at or around day 14, whereas higher level of *Lox* at day 28 corresponds to higher level of *Col1a2* and *Col3a1* (Figure 4(m) to (p)). In the rat skin healing studies, the *Lox* mRNA level reached a peak by day 3 after injury, which was earlier than that of type III collagen, and continued at a high level until day 22. The type III collagen mRNA level began to rise from day 3 and had intensely increased by day 22.[39] Transfection studies show that the *Lox* and *Col1a1* promoters may be regulated by similar negative and positive cis-acting elements, which include TGF-β response element reported for rat *Col1a1*[40] and for mouse *Col1a2* promoters.[41] In vitro studies have shown that hrTGFβ1 causes an increase in *Lox* mRNA expression in murine tail tenocytes.[42]

Versican (VCAN), a large chondroitin sulfate proteoglycan, is a component of ECM found in a number of tissues.[43] During healing, when the inflammation is turning off, epithelialization and matrix formation are initiated by migrating proliferating fibroblasts that lay down a provisional matrix bed rich in versican among other molecules. As this bed is degraded by MMPs, myofibroblasts go into apoptosis, and the structure and function of the tissue are restored. In patellar tendinosis, an increased deposition of versican has been reported.[44] Decorin (DCN) is an ECM chondroitin/dermatan sulfate small leucine-rich proteoglycan (SLRP). The structural features of decorin provide its critical role in ECM assembly. Wound healing is delayed in mice lacking decorin.[45] In myocardial infarction, *Vcan* and *Dcn* mRNA expression showed reverse trend in their expression over healing. *Vcan* mRNA expression was transiently induced in the infiltrating monocytes as shown by

an increase at 6 h through day 7 and then decreased sharply till day 28, whereas *Dcn* mRNA increased that replaced the decreasing *Vcan* mRNA expression.[46] In this study, a similar reverse relation of *Vcan* and *Dcn* mRNA expression in FDL tendon graft healing was obtained. Versican mRNA expression was significantly higher at days 7 and 14 and was on decline thereafter, whereas decorin mRNA expression was significantly higher at later days at days 21, 28, and 35 (Figure 5(a) and (b)). This study supports the notion that versican (a component of provisional matrix) is replaced by decorin, which is required during matrix assembly, collagen fibrillogenesis, and remodeling.

Biglycan and decorin belong to the SLRPs class I subfamily. Both contain 12 leucine-rich repeats (LRRs). Biglycan has two attached glycosaminoglycan (GAG) chains and decorin has one. The GAG can be either chondroitin sulfate or dermatan sulfate depending on the tissue origin. Biglycan binds collagen type I in the gap zone of the fibrils, and decorin competes for that interaction.[47] Decorin has a high-affinity collagen-binding site in the sixth LRR.[48] The effects of the two GAG chains present on biglycan are reasonably different from the single GAG of decorin. The switch in expression levels of these SLRPs during tendon development is demonstrated by the fact that decorin protein increases gradually with development from P4 to P30 by 70%, whereas biglycan core protein decreases from P4 to P30 by 50% in flexor tendon. The stage in normal tendon development (P30) where decorin peaked and biglycan decreased to its lowest level was assessed in early fibril assembly, and decorin persists until thick fibrils are formed.[49] The two GAG chains are proper organizers in the formation of early fibrils, perhaps by controlling the multitudes of small fibrils that would otherwise assemble in an uncontrolled manner. Biglycan, and not decorin, is upregulated by 100% in compressed tendons, where mechanical stress induces collagen fibrillogenesis.[50]

Significantly higher mRNA expression of *Bgn* during healing indicates its role in collagen fibrillogenesis process in this study (Figure 5(c)). In the rat healing model in in vitro wound chambers, *Bgn* mRNA shows higher level of expression during healing from days 12 to 22 in a 22-day study.[51] By using biglycan-deficient mice, Corsi et al.[52] were able to show altered collagen fibrillogenesis in tail tendon as compared to WT. Tendon from 2-month-old male hemizygous $Bgn^{-/0}$ mice is abnormally shaped and unusually large diameter fibrils.[52] Hiroyuki et al.[53] were able to demonstrate that biglycan deficiency adversely affects the mechanical property of the healing bone insertion site of the patellar tendon fibers after 4 weeks post surgery in mice. Collagen fibril diameter distribution was disturbed in mutant mice.

Decorin-deficient mice show abnormal collagen fibrils in FDL and tail tendon, the effect is more severe in tail tendon indicating differential role of this proteoglycan in different tendons.[49,52,54] Reduced mechanical properties were recorded in FDL tendon in mature decorin-deficient mice.[49] In another interesting study, on the same mutant gene, Ilkhani-Pour et al. showed that injured decorin-deficient Achilles tendons heal better than WT tendons. Injured $Dcn^{-/-}$ tendons showed decreased tendon cross-section area, increased linear modulus, decreased tan(δ), and increased dynamic modulus $|E^*|$ compared to WT Achilles tendon. Authors suggested that the deletion of decorin during tendon healing might have reduced scarring and improved collagen fibrillogenesis by allowing the formation of more mechanically stable collagen fibrils.[55] Decorin mRNA expression was significantly higher at later days at days 21, 28, and 35 (Figure 5(b)), indicating its possible role in collagen fibrillogenesis and adhesion formation.

Decorin also has the ability to bind to TGFβ1, which is involved in the regulation of cell proliferation, differentiation, ECM production, wound healing, and tissue repair.[56,57] TGF-β is of crucial importance in triggering excessive formation and deposition of connective tissue matrix molecules. Decorin–TGFβ1 complex formation may lead to inactivation of some cytokines and TGFβ1 itself in connective tissue.[58–60] To test if scar formation can be prevented by controlling decorin expression in tenocytes, Achilles tendon cells from rabbit were transfected with antisense decorin, and the authors found that it suppressed Tgfβ1 production. Scar formation could be prevented by controlling decorin expression in tendinocytes.[61]

Periostin, a secreted cell adhesion protein, is a matricellular protein.[62] Periostin is predominantly expressed in collagen-rich fibrous connective tissues that are subjected to constant mechanical stress including heart valves, tendons, and periodontal ligament. Periostin binds to collagen I and plays a role in collagen fibrillogenesis as also evidenced by *Postn*-KO mice.[63] This study shows, for the first time, that periostin plays a role in healing FDL tendon graft in mouse. Periostin mRNA expression was increased at day 7 and remained significantly high until day 28 (Figure 5(d)), indicating its role in tendon maturation, collagen fibril arrangement, and remodeling events.

Tenascins are a family of ECM proteins that evolved in early chordates. There are four family members: tenascin X, R, W (new name N), and C. Tenascin X associates with type I collagen. In contrast, tenascin R is concentrated in perineuronal nets. The expression of tenascin C and tenascin N/W is developmentally regulated and both are expressed during the disease state.[64] Tenascin C is an elastic ECM protein that can be stretched multiple times its resting length. Thus, it provides elasticity for the musculoskeletal tissue undergoing repair.[65] In normal adult tendons, it is expressed predominately in regions transmitting high levels of mechanical force, such as the myotendinous and osteotendinous junctions.[66,67,68] Tenascin C is abundant in the tendon pericellularly and around the collagen fibers of the tendon belly.[66] The protein is expressed around the cells

and collagen fibers of the Achilles tendon.[64] In addition, Järvinen et al.[65,68] have shown that expression of the *TNC* gene is regulated in a dose-dependent manner by mechanical loading in tendons. In this study, only the early induction of *Tnc* takes place in the granulation tissue, but due to the immobility caused by the tendon transection proximally, there is no expression of *Tnc* at the later stages of healing. Healthy tendons express a small 200-kDa tenascin C isoform, while degenerating tendons express a functionally distinct larger 300-kDa isoform.[69] Ireland et al.[70] and Mokone et al.[71] have reported an increase in tenascin C expression in biopsy samples of chronic Achilles tendinopathies. Tenascin C mRNA expression is upregulated in FDL tendon graft healing at day 7 at the time of fibroplasia and granulation tissue formation in which wound contracts and collagen deposits. This is further supported by the recent finding that in vitro Tenascin C-deficient lung fibroblasts expressed less α-SMA and deposited less collagen I into the matrix.[72] In the wounded skin, staining pattern of tenascin, in dermis, gradually increased from the third day and reached peak level at about 8 days after wounding. At this stage, it was enriched in the granulation tissue, and its distribution corresponded to the middle of the newly formed collagen fibrils.[73]

Thrombospondin-2 (Thbs2 or Tsp2) belongs to a family of multimeric, ECM, secreted modular glycoproteins and functions as a matricellular protein to influence cell function by modulating cell–matrix interactions.[74] It is expressed in organized connective tissues including ligaments and blood vessels during murine embryonic development.[75] Thrombospondin-2-deficient mice display fragile skin associated with disordered dermal collagen fibrillogenesis and increased vascular density.[76] Early postnatal flexor tendon show distinct abnormality in fibroblast–collagen fibril interactions in *Tsp2*-KO tissues.[77] The structurally abnormal collagen fibrils, detected in skin, appear to be the consequence of the defective adhesion demonstrated by dermal fibroblasts in culture that, in turn, result from increased matrix metalloproteinase-2 (MMP-2) production by these cells.[76] The study show, for the first time, that thrombospondin-2 plays a role in murine FDL tendon graft healing. Expression of *Thbs2* mRNA was significantly higher at days 14 to 28 (Figure 5(f)), coinciding with peak angiogenesis events (Figure 1) supporting Iruela-Arispe et al.'s[75] studies and coinciding with higher expression profile of collagens for its role in maturation and remodeling events (Figures 4(m) to (o) and 5(f)).

A secreted and an ECM-associated metalloprotease with three thrombospondin motifs, ADAMTS-1, mediate cleavage release of polypeptides generating a pool of antiangiogenic fragments from matrix-bound THBS-1 and THBS-2.[78] It appears that ADAMTS-1 and thrombospondins may play an interdependent role in regulating antiangiogenesis during tendon graft healing. *Thbs2* mRNA expression level, in the current FDL tendon graft healing study, was significantly higher during peak angiogenesis event at days 14, 21, and 28 (Figures 1 and 5(f)), whereas *Adamts1* mRNA expression showed a reverse trend being the lowest at days 21 and 28 (Figure 5(g)). How and whether these two molecules regulate angiogenesis in tendon graft healing is an open question.

The relevance of MMP-8 in wound repair is suggested by the fact that this neutrophil protease is the main collagenase produced in healing wounds.[79] Mouse deficient in MMP-8 shows a significant delay in wound closure with an altered inflammatory response in their wounds.[80] In the current FDL tendon graft healing studies, MMP-8 appears to be actively involved. *Mmp8* mRNA expression was maximum at day 3 and then decreases gradually to low level by day 35 (Figure 5(h)), indicating its role in inflammatory event of tendon healing. Thus, this study shows that MMP-8 plays a role in FDL tendon graft healing at inflammatory phase.

In rabbit flexor tendon injury, the *Mmp13* mRNA expression levels, evaluated in tendon and tendon sheath at several time-points (days 3, 6, 21, and 42), remained upregulated during the study period.[27] *Mmp13* mRNA expression was biphasic, with peak activities at days 15 and 37 of surgery after skin injury by scalpel or laser.[81] In the current FDL tendon graft healing, mRNA expression of *Mmp13* also shows two major significantly higher peaks at days 14 and 35 and two minor significantly higher peaks at days 21 and 28 (Figure 5(i)), indicating its role in tissue remodeling during healing process.

The MMP-2 and MMP-9 have multiple substrates including gelatins, collagenous and noncollagenous ECM, and nonstructural ECM components.[82] Various studies have shown that MMP-2 and MMP-9 play a role during skin wound healing and as well as in tendon healing. In the current FDL tendon graft healing studies, *Mmp2* mRNA expression showed its highest peak at days 14 and 35 (Figure 5(j)), whereas *Mmp9* mRNA level was highest at day 3 (Figure 5(k)), indicating that MMP-2 is involved in biphasic manner during remodeling phase and MMP-9 plays a role in inflammatory and early granular tissue formation. In a rat FDL laceration and repair model, MMP-2 peaked at days 14 and 28 and MMP-9 was highest at days 7 and 14.[37] In brief, this study shows that both *Mmp2* and *Mmp9* are involved in FDL tendon graft healing process.

The membrane-bound matrix metalloproteinase, MMP-14, mediates pericellular proteolysis of ECM components and plays a role in cellular remodeling of the surrounding matrix. The enzyme has multiple substrates, including gelatins; collagen I, II, III; proteoglycans; fibronectin; tenascin; fibrinogen; Pro-MMP-2; and Pro-MMP-13.[82] Among others, one of the phenotypes of *Mmp14*-KO is fibrosis of soft tissues due to ablation of collagenolytic activity that is essential for remodeling of connective tissues.[83] It was shown that MMP-14 plays a role in flexor tendon healing. In rat flexor tendon healing process, *Mmp14* mRNA

expression was higher at days 7, 14, 21, and 28 indicating its role in collagen degradation as well as in remodeling.[37] In the current FDL tendon graft healing study, *Mmp14* mRNA was significantly higher at days 7, 14, 21, and 35 (Figure 5(l)), indicating its role in collagen degradation during granulation as well as its role in FDL tendon graft remodeling and adhesions. In short, this study shows that MMP-14 plays an important role in FDL tendon graft healing.

Canonical BMP signaling pathway involves SMAD9 or SMAD8. In this pathway, SMAD 1/5/8 are phosphorylated by BMP receptors. The SMAD8 has been shown to be important in inducing neotendon formation from mesenchymal stem cells and has been proposed to play a role in tendon repair.[84] The mRNA expression levels for *Smad8* were significantly higher at day 14 through day 35 (Figure 5(m)), indicating that SMAD8 plays a role in FDL tendon graft healing. In an induced mesenchyme to tenocyte differentiation study, knockdown of *Smad8* prevented the expression of tenocyte markers.[85]

Scleraxis (SCX) is a specific marker for all the connective tissues that mediate attachment of muscle to bone, including the limb tendons, and its expression marks the progenitor cell populations for these tissues.[86] Tendon healing is a regenerative process and tendon progenitor cells are expected to play a role in healing process. Higher *Scx* mRNA expression during FDL tendon graft healing was observed, indicating that scleraxis plays a role in healing process (Figure 5(n)). In a murine patellar tendon injury model, *Scx* mRNA expression was measured at 1-, 4- and 8-week time-points. The authors observed increased expression at 4- and 8-week time-points.[88] Rats undergoing unilateral detachment and repair of the supraspinatus tendon and receiving Ad-*Scx*-transduced mesenchyme stem cells at the repair site showed improved tensile strength assessed at 2 and 4 weeks.[87]

Mohawk homeobox (MKX) is a member of the "Three Amino acid Loop Extension" superclass of atypical homeobox genes that are expressed in developing tendons.[89] *Mkx* mRNA is strongly expressed in differentiating tendon cells during embryogenesis and in the tendon sheath cells in postnatal stages.[90] Mice deleted in *Mkx* gene show smaller collagen fibril diameter, reduction in tendon mass, and down-regulation of type I collagen content.[89] These studies identify that mohawk homeobox is an important regulator of tendon development. This study shows, for the first time, that mohawk homeobox is important in tendon healing process. Gene expression of *Mkx* mRNA determined at day 3, 21, and 35 was increased significantly at day 21 and 35 as compared to day 3 expression (Figure 5(o)), which indicates that the mohawk homeobox plays a role in FDL tendon graft healing process.

Tubulin polymerization-promoting protein 3 (TPPP3) is a member of the tubulin polymerization-promoting protein family.[91] In tendons, TPPP3 is expressed in cells at the circumference of the developing tendons, likely the progenitors of connective tissues that surround tendons: the tendon sheath, epitenon, and paratenon. These tissues form an elastic sleeve around tendons and provide lubrication to minimize friction between tendons and surrounding tissues during gliding. TPPP3 is the first molecular marker of the tendon sheath.[90] Higher mRNA expression at days 21 and 35 indicates that it may play a role in the remodeling of tendon sheath during FDL tendon graft healing (Figure 5(p)).

Gene expression profile, during tendon graft healing and scar and adhesion formation, indicated that all the genes studied participated in the process. Some of the genes, first time studied in tendon graft healing (*Alk1, Postn, Tnc, Tppp3*, and *Mkx*), can be a potential target for therapy to reduce scars and reduce or inhibit adhesion formation.

Conclusion

By using a mouse model for FDL tendon graft repair using Rosa26/+ mouse as an allograft donor and WT mouse as a recipient, this investigation reports that tendon graft healing takes place in an interactive environment created by host tendon, donor graft, and host surrounding tissue in an intrasynovial FDL tendon healing model. Manipulating this interactive environment, by therapeutical approaches, may lead to solutions for reducing scar formation and thus for reducing or inhibiting adhesion formations. Gene expression profile during tendon healing and scar and adhesion formation indicated that all the genes studied here participated in one or more of these processes. Some of the genes, first time studied in tendon healing (*Alk1, Postn, Tnc, Tppp3 and Mkx*), will be further investigated if they can be of some therapeutical value in reducing scars and preventing adhesion formation.

Acknowledgements

The author is grateful to Dr. Tony Chen and Dr. Alayna Loiselle for sharing their research knowledge in the project. The author thanks Dr Justin Jacobson for teaching mouse tendon surgery, Dr Chao Xie for teaching cryosectioning and microtome operation, Dr Matthew Hilton for providing working lab protocols for cryosections for X-gal staining, Dr Alicia Clementi for advising real-time PCR technical tips, Dr Awad for occasional discussions on the project, Ms Cushing for ordering lab supplies, Bonnie for administration work, Susan for autoclaving glasswares, and Donna for providing initial two breeding pairs of animals from her mouse colony. Thanks to Dr Hani Awad, Dr Regis O'Keefe, and Prof. Eddie Schwarz for their continuous support in tendon research and funding for research. This work was presented as a poster and as an oral presentation at 2012 ORS meeting, San Francisco, CA, USA, and was among the work selected for New Investigator Research Award Presentations, NIRA-2, abstract no. 335.

Declaration of conflicting interests

The author declares that there is no conflict of interest.

Funding

This research received financial support from Center for Musculoskeletal Research at the University of Rochester, Rochester, NY, USA.

References

1. Taras JS and Lamb MJ. Treatment of flexor tendon injuries: surgeons' perspective. *J Hand Ther* 1999; 12: 141–148.
2. Lilly SI and Messer TM. Complications after treatment of flexor tendon injuries. *J Am Acad Orthop Surg* 2006; 14: 387–396.
3. Stark HH, Anderson DR, Zemel NP, et al. Bridge flexor tendon grafts. *Clin Orthop Relat Res* 1989; 242: 51–59.
4. Seiler JG. 3rd, Chu CR, Amiel D, et al. The Marshall R. Urist Young Investigator Award. Autogenous flexor tendon grafts. Biologic mechanisms for incorporation. *Clin Orthop Relat Res* 1997; 345: 239–247.
5. Boyer MI. Flexor tendon biology. *Hand Clin* 2005; 21: 159–166.
6. Soriano P. Generalized lacZ expression with the ROSA26 Cre reporter strain. *Nat Genet* 1999; 21: 70–71.
7. Hasslund S, Jacobson JA, Dadali T, et al. Adhesions in a murine flexor tendon graft model: autograft versus allograft reconstruction. *J Orthop Res* 2008; 26: 824–833.
8. Wu YF, Chen CH, Cao Y, et al. Molecular events of cellular apoptosis and proliferation in the early tendon healing period. *J Hand Surg Am* 2010; 35: 2–10.
9. Wong JK, Lui YH, Kapacee Z, et al. The cellular biology of flexor tendon adhesion formation: an old problem in a new paradigm. *Am J Pathol* 2009; 175: 1938–1951.
10. Kobayashi M, Watanabe N, Oshima Y, et al. The fate of host and graft cells in early healing of bone tunnel after tendon graft. *Am J Sports Med* 2005; 33: 1892–1897.
11. Crippa MP. Urokinase-type plasminogen activator. *Int J Biochem Cell Biol* 2007; 39: 690–694.
12. Smith PC and Martínez J. Differential uPA expression by TGF-beta1 in gingival fibroblasts. *J Dent Res* 2006; 85: 150–155.
13. Xia W, De Bock C, Murrell GA, et al. Expression of urokinase-type plasminogen activator and its receptor is upregulated during tendon healing. *J Orthop Res* 2003; 21: 819–825.
14. Chan JC, Duszczyszyn DA, Castellino FJ, et al. Accelerated skin wound healing in plasminogen activator inhibitor-1-deficient mice. *Am J Pathol* 2001; 159: 1681–1688.
15. Weiler A, Unterhauser FN, Bail HJ, et al. Alpha-smooth muscle actin is expressed by fibroblastic cells of the ovine anterior cruciate ligament and its free tendon graft during remodeling. *J Orthop Res* 2002; 20: 310–317.
16. Menetrey J, Laumonier T, Garavaglia G, et al. α-smooth muscle actin and TGF-β receptor I expression in the healing rabbit medial collateral and anterior cruciate ligaments. *Injury* 2011; 42: 735–741.
17. O'Malley Y, Zhao W, Barcellos-Hoff MH, et al. Radiation-induced alterations in rat mesangial cell Tgfb1 and Tgfb3 gene expression are not associated with altered secretion of active Tgfb isoforms. *Radiation Res* 1999; 152: 622–628.
18. Frank S, Madlener M and Werner S. Transforming growth factors beta1, beta2, and beta3 and their receptors are differentially regulated during normal and impaired wound healing. *J Biol Chem* 1996; 271: 10188–10193.
19. Douglas HE. Tgf-β in wound healing: a review. *J Wound Care* 2010; 19: 403–406.
20. Massague J. How cells read TGF-β signals. *Nat Rev Mol Cell Biol* 2000; 1: 169–178.
21. Lebrin F, Deckers M, Bertolino P, et al. TGF-beta receptor function in the endothelium. *Cardiovasc Res* 2005; 65: 599–608.
22. Marchuk DA. The molecular genetics of hereditary hemorrhagic telangiectasia. *Chest* 1997; 111: 79S–82S.
23. Seki T, Hong KH, Yun J, et al. Isolation of a regulatory region of activin receptor-like kinase1gene sufficient for arterial endothelium-specific expression. *Circ Res* 2004; 94: e72–e77.
24. Ngo M, Pham H, Longaker MT, et al. Differential expression of transforming growth factor-beta receptors in a rabbit zone II flexor tendon wound healing model. *Plast Reconstr Surg* 2001; 108: 1260–1267.
25. Sciore P, Boykiw R and Hart DA. Semiquantitative reverse transcription-polymerase chain reaction analysis of mRNA for growth factors and growth factor receptors from normal and healing rabbit medial collateral ligament tissue. *J Orthop Res* 1998; 16: 429–437.
26. Tsubone T, Moran SL, Amadio PC, et al. Expression of growth factors in canine flexor tendon after laceration in vivo. *Ann Plast Surg* 2004; 53: 393–397.
27. Berglund ME, Hart DA, Reno C, et al. Growth factor and protease expression during different phases of healing after rabbit deep flexor tendon repair. *J Orthop Res* 2011; 29: 886–892.
28. Itoh N and Ornitz DM. Fibroblast growth factors: from molecular evolution to roles in development, metabolism and disease. *J Biochem* 2011; 149: 121–130.
29. Ortega S, Ittmann M, Tsang SH, et al. Neuronal defects and delayed wound healing in mice lacking fibroblast growth factor-2. *Proc Natl Acad Sci U S A* 1998; 95: 5672–5677.
30. Thomopoulos S, Das R, Sakiyama-Elbert S, et al. bFGF and PDGF-BB for tendon repair: controlled release and biologic activity by tendon fibroblasts in vitro. *Ann Biomed Eng* 2010; 38: 225–234.
31. Tang JB, Cao Y, Zhu B, et al. Adeno-associated virus-2-mediated bFGF gene transfer to digital flexor tendons significantly increases healing strength. An in vivo study. *J Bone Joint Surg Am* 2008; 90: 1078–1089.
32. Chen D, Zhao M and Mundy GR. Bone morphogenetic proteins. *Growth Factors* 2004; 22: 233–241.
33. Wolfman NM, Hattersley G, Cox K, et al. Ectopic induction of tendon and ligament in rats by growth and differentiation factors 5, 6, and 7, members of the TGF-beta gene family. *J Clin Invest* 1997; 100: 321–330.
34. Mikic B. Multiple effects of GDF-5 deficiency on skeletal tissues: implications for therapeutic bioengineering. *Ann Biomed Eng* 2004; 32: 466–476.
35. Aspenberg P and Forslund C. Enhanced tendon healing with GDF 5 and 6. *Acta Orthop Scand* 1999; 70: 51–54.
36. Chhabra A, Tsou D, Clark RT, et al. GDF-5 deficiency in mice delays Achilles tendon healing. *J Orthop Res* 2003; 21: 826–835.
37. Oshiro W, Lou J, Xing X, et al. Flexor tendon healing in the rat: a histologic and gene expression study. *J Hand Surg Am* 2003; 28: 814–823.

38. Dahlgren LA, Mohammed HO and Nixon AJ. Temporal expression of growth factors and matrix molecules in healing tendon lesions. *J Orthop Res* 2005; 23: 84–92.
39. Fushida-Takemura H, Fukuda M, Maekawa N, et al. Detection of lysyl oxidase gene expression in rat skin during wound healing. *Arch Dermatol Res* 1996; 288: 7–10.
40. Ritzenthaler JD, Goldstein RH, Fine A, et al. Transforming-growth-factor-β activation elements in the distal promoter regions of the rat α1 type I collagen gene. *Biochem J* 1991; 280: 157–162.
41. Rossi P, Karsenty G, Roberts AB, et al. A nuclear factor 1 binding site mediates the transcriptional activation of a type I collagen promoter by transforming growth factor-β. *Cell* 1988; 52: 405–414.
42. Juneja SC, Reynolds D, Awad HA, et al. Tendon/ligament defect in Mds1 knockout mouse. In: *Orthopedic Research Society (ORS) meeting*, Long Beach CA, USA, 13–16 January 2011, poster no. 1620. Rosemont, IL: ORS.
43. Wight TN. Versican: a versatile extracellular matrix proteoglycan in cell biology. *Curr Opin Cell Biol* 2002; 14: 617–623.
44. Scott A, Lian Ø, Roberts CR, et al. Increased versican content is associated with tendinosis pathology in the patellar tendon of athletes with jumper's knee. *Scand J Med Sci Sports* 2008; 18: 427–435.
45. Järveläinen H, Puolakkainen P, Pakkanen S, et al. A role for decorin in cutaneous wound healing and angiogenesis. *Wound Repair Regen* 2006; 14: 443–452.
46. Toeda K, Nakamura K, Hirohata S, et al. Versican is induced in infiltrating monocytes in myocardial infarction. *Mol Cell Biochem* 2005; 280: 47–56.
47. Schönherr E, Hausser H, Beavan L, et al. Decorin-type I collagen interaction. Presence of separate core protein-binding domains. *J Biol Chem* 1995; 270: 8877–8883.
48. Kalamajski S, Aspberg A and Oldberg A. The decorin sequence SYIRIADTNIT binds collagen type I. *J Biol Chem* 2007; 282: 16062–16067.
49. Zhang G, Ezura Y, Chervoneva I, et al. Decorin regulates assembly of collagen fibrils and acquisition of biomechanical properties during tendon development. *J Cell Biochem* 2006; 98: 1436–1449.
50. Robbins JR, Evanko SP and Vogel KG. Mechanical loading and TGF-beta regulate proteoglycan synthesis in tendon. *Arch Biochem Biophys* 1997; 342: 203–211.
51. Simeon A, Wegrowski A, Bontemps Y, et al. Expression of glycosaminoglycans and small proteoglycans in wounds: modulation by the tripeptide-copper complex glycyl-L-histidyl-L-lysine-Cu(2+). *J Invest Dermatol* 2000; 115: 962–968.
52. Corsi A, Xu T, Chen XD, et al. Phenotypic effects of biglycan deficiency are linked to collagen fibril abnormalities, are synergized by decorin deficiency, and mimic Ehlers-Danlos-like changes in bone and other connective tissues. *J Bone Miner Res* 2002; 17: 1180–1189.
53. Hiroyuki Y, Hiromichi F, Wataru A, et al. Patellar tendon strength of a specific protein-knockout mouse. Effects of biglycan on the mechanical property of biological fibrous tissues. *Nihon Kikai Gakkai Kanto Shibu Sokai Koen Ronbunshu* 2005; 11: 475–476.
54. Danielson KG, Baribault H, Holmes DF, et al. Targeted disruption of decorin leads to abnormal collagen fibril morphology and skin fragility. *J Cell Biol* 1997; 136: 729–743.
55. Ilkhani-Pour S, Voleti PB, Buckley MR, et al. Achilles tendon repair response to injury is enhanced by the absence of decorin. In: Orthopedic Research Society (ORS), annual meeting, San Antonio, TX, 26–29 January 2013, poster no. 0616. Rosemont, IL: ORS.
56. Moustakas A, Pardali K, Gaal A, et al. Mechanisms of TGF-beta signaling in regulation of cell growth and differentiation. *Immunol Lett* 2002; 82: 85–91.
57. Comalada M, Cardó M, Xaus J, et al. Decorin reverses the repressive effect of autocrine-produced TGF-beta on mouse macrophage activation. *J Immunol* 2003; 170: 4450–4456.
58. Border WA, Noble NA, Yamamoto T, et al. Natural inhibitor of transforming growth factor-beta protects against scarring in experimental kidney disease. *Nature* 1992; 360: 361–364.
59. Rapraeger AC, Krufka A and Olwin BB. Requirement of heparan sulfate for bFGF-mediated fibroblast growth and myoblast differentiation. *Science* 1991; 252: 1705–1708.
60. Olwin BB and Rapraeger A. Repression of myogenic differentiation by aFGF, bFGF, and K-FGF is dependent on cellular heparan sulfate. *J Cell Biol* 1992; 118: 631–639.
61. Hosaka Y, Kirisawa R, Mafune N, et al. Downregulation of decorin and transforming growth factor-beta1 by decorin gene suppression in tendinocytes. *Connect Tissue Res* 2005; 46: 18–26.
62. Hamilton DW. Functional role of periostin in development and wound. *J Cell Commun Signal* 2008; 2: 9–17.
63. Norris RA, Damon B, Mironov V, et al. Periostin regulates collagen fibrillogenesis and the biomechanical properties of connective tissues. *J Cell Biochem* 2007; 101: 695–711.
64. Chiquet-Ehrismann R and Tucker RP. Tenascins and the importance of adhesion modulation. *Cold Spring Harb Perspect Biol* 2011; 10: 7–19.
65. Järvinen TA, Józsa L, Kannus P, et al. Mechanical loading regulates the expression of tenascin-C in the myotendinous junction and tendon but does not induce de novo synthesis in the skeletal muscle. *J Cell Sci* 2003; 116: 857–866.
66. Chiquet M and Fambrough DM. Chick myotendinous antigen. II. A novel extracellular glycoprotein complex consisting of large disulfide-linked subunits. *J Cell Biol* 1984; 98: 1937–1946.
67. Kannus P, Jozsa L, Jarvinen TA, et al. Location and distribution of non-collagenous matrix proteins in musculoskeletal tissues of rat. *Histochem J* 1998; 30: 799–810.
68. Järvinen TA, Jozsa L, Kannus P, et al. Mechanical loading regulates tenascin-C expression in the osteotendinous junction. *J Cell Sci* 1999; 112: 3157–3166.
69. Riley GP, Harrall RL, Cawston TE, et al. Tenascin-C and human tendon degeneration. *Am J Pathol* 1996; 149: 933–943.
70. Ireland D, Harrall R, Curry V, et al. Multiple changes in gene expression in chronic human Achilles tendinopathy. *Matrix Biol* 2001; 20: 159–169.
71. Mokone GG, Gajjar M, September AV, et al. The guanine-thymine dinucleotide repeat polymorphism within the tenascin-C gene is associated with Achilles tendon injuries. *Am J Sports Med* 2005; 33: 1016–1021.
72. Carey WA, Taylor GD, Dean WB, et al. Tenascin-C deficiency attenuates TGF-β-mediated fibrosis following murine lung injury. *Am J Physiol Lung Cell Mol Physiol* 2010; 299: L785–L793.

73. Chuong CM and Chen HM. Enhanced expression of neural cell adhesion molecules and tenascin (cytotactin) during wound healing. *Am J Pathol* 1991; 138: 427–440.
74. Bornstein P. Thrombospondins as matricellular modulators of cell function. *J Clin Invest* 2001; 107: 929–934.
75. Iruela-Arispe ML, Liska DJ and Sage EH.. Differential expression of thrombospondin 1, 2, and 3 during murine development. *Dev Dyn* 1993; 197: 40–56.
76. Kyriakides TR, Zhu YH, Smith LT, et al. Mice that lack thrombospondin 2 display connective tissue abnormalities that are associated with disordered collagen fibrillogenesis, an increased vascular density, and a bleeding diathesis. *J Cell Biol* 1998; 140: 419–430.
77. Bornstein P, Kyriakides TR, Yang Z, et al. Thrombospondin 2 modulates collagen fibrillogenesis and angiogenesis. *J Investig Dermatol Symp Proc* 2000; 5: 61–66.
78. Lee NV, Sato M, Annis DS, et al. ADAMTS1 mediates the release of antiangiogenic polypeptides from TSP1 and 2. *EMBO J* 2006; 25: 5270–5283.
79. Nwomeh BC, Liang HX, Cohen IK, et al. MMP-8 is the predominant collagenase in healing wounds and nonhealing ulcers. *J Surg Res* 1999; 81: 189–195.
80. Gutiérrez-Fernández A, Inada M, Balbín M, et al. Increased inflammation delays wound healing in mice deficient in collagenase-2 (MMP-8). *FASEB J* 2007; 21: 2580–2591.
81. Wu N, Jansen ED and Davidson JM. Comparison of mouse matrix metalloproteinase 13 expression in free-electron laser and scalpel incisions during wound healing. *J Invest Dermatol* 2003; 121: 926–932.
82. Pasternak B. *Towards surgical use of matrix metalloproteinase biology*. Medical Dissertations, Linkoping University, Sweden, 2008.
83. Holmbeck K, Bianco P, Caterina J, et al. MT1-MMP-deficient mice develop dwarfism, osteopenia, arthritis, and connective tissue disease due to inadequate collagen turnover. *Cell* 1999; 99: 81–92.
84. Hoffmann A, Pelled G, Turgeman G, et al. Neotendon formation induced by manipulation of the Smad8 signalling pathway in mesenchymal stem cells. *J Clin Invest* 2006; 116: 940–952.
85. Ramcharan M, Li Z, Lee JY, et al. Smad8 activation: common signaling pathway that may be required for BMP12 and mechanical loading induced mesenchymal stem cell teno-differentiation. In: Orthopedic Research Society (ORS) meeting, New Orleans, LA, USA, 6–9 March, 2010, poster no. 1097. Rosemont, IL: ORS.
86. Schweitzer R, Chyung JH and Murtaugh LC. Analysis of the tendon cell fate using Scleraxis, a specific marker for tendons and ligaments. *Development* 2001; 128: 3855–3866.
87. Gulotta LV, Kovacevic D, Packer JD, et al. Bone marrow-derived mesenchymal stem cells transduced with Scleraxis improve rotator cuff healing in a rat model. *Am J Sports Med* 2011; 39: 1282–1289.
88. Scott A, Sampaio A, Abraham T, et al. Scleraxis expression is coordinately regulated in a murine model of patellar tendon injury. *J Orthop Res* 2011; 29: 289–296.
89. Ito Y, Toriuchi N, Yoshitaka T, et al. The Mohawk homeobox gene is a critical regulator of tendon differentiation. *Proc Natl Acad Sci U S A* 2010; 107: 10538–10542.
90. Liu W, Watson SS, Lan Y, et al. The atypical homeodomain transcription factor Mohawk controls tendon morphogenesis. *Mol Cell Biol* 2010; 30: 4797–4807.
91. Staverosky JA, Pryce BA, Watson SS, et al. Tubulin polymerization-promoting protein family member 3, Tppp3, is a specific marker of the differentiating tendon sheath and synovial joints. *Dev Dyn* 2009; 238: 685–692.